Optical properties of $V_{1-x}Cr_xO_2$ compounds under high pressure

C. Marini,[1,2] E. Arcangeletti,[1] D. Di Castro,[1] L. Baldassare,[1] A. Perucchi,[1] S. Lupi,[1] L. Malavasi,[3] L Boeri,[4] E. Pomjakushina,[5,6] K. Conder,[5] and P. Postorino[1]

[1]*"Coherentia" CNR-INFM and Dipartimento di Fisica, Universitá di Roma La Sapienza, Piazzale Aldo Moro 2, I-00185 Roma, Italy*

[2]*Dipartimento di Fisica "E. Amaldi," Universitá degli Studi Roma Tre, via della Vasca Navale 84, 00146 Roma, Italy and "unitá CNISM Roma1," Universitá di Roma La Sapienza, Piazzale Aldo Moro 2, I-00185 Roma, Italy*

[3]*Dipartimento di Chimica Fisica "M. Rolla," INSTM and IENI-CNR, Universitá di Pavia, Viale Taramelli 16, I-27100 Pavia, Italy*

[4]*Max-Planck Institut für Festkörperforschung, Heisenbergstrasse 1, D-70569 Stuttgart, Germany*

[5]*Laboratory for Developments and Methods, Paul Scherrer Institute, CH-5232 Villigen PSI, Switzerland*

[6]*Laboratory for Neutron Scattering, Paul Scherrer Institute and ETH Zurich, CH-5232 Villigen PSI, Switzerland*

(Received 8 April 2008; published 16 June 2008)

Raman and infrared transmission and reflectivity measurements were carried out at room temperature and high pressure (0–15 GPa) on $V_{1-x}Cr_xO_2$ compounds. Raman spectra were collected at ambient conditions on the $x=0.007$ and 0.025 materials, which are characterized by different insulating monoclinic phases ($M3$ and $M2$, respectively), while infrared spectra were collected on the $x=0.025$ sample only. The present data were compared with companion results on undoped VO_2 [E. Arcangeletti *et al.*, Phys. Rev. Lett. **98**, 196406 (2007)], which is found at ambient conditions in a different, third insulating monoclinic phase, named $M1$. This comparison allowed us to investigate the effects of different extents of structural distortions (Peierls distortion) on the lattice dynamics and the electronic properties of this family of compounds. The pressure dependence of the Raman spectrum of VO_2 and Cr-doped samples shows that all the systems retain the monoclinic structure up to the highest explored pressure, regardless the specific monoclinic structure ($M1$, $M2$, and $M3$) at ambient condition. Moreover, the Raman spectra of the two Cr-doped samples, which exhibit an anomalous behavior over the low-pressure range ($P<8$ GPa), merge into that of VO_2 in the high-pressure regime and are all found into a common monoclinic phase (a possible fourth kind phase). Combining Raman and infrared results on both the VO_2 and the present data, we found that a common metallic monoclinic phase appears accessible in the high-pressure regime at room temperature for both undoped and Cr-doped samples independently of the different extents of Peierls distortion at ambient conditions. This finding differs from the behavior observed at ambient pressure, where the metallic phase is found only in conjunction with the rutile structure. The whole of these results suggests a major role of the electron correlations, rather than of the Peierls distortion, in driving the metal-insulator transition in vanadium dioxide systems, thus opening to new experimental and theoretical queries.

DOI: 10.1103/PhysRevB.77.235111 PACS number(s): 71.30.+h, 62.50.−p, 78.30.−j, 63.20.kd

I. INTRODUCTION

Since the first observation of the metal to insulator transition (MIT) in several vanadium oxides, these materials attracted considerable interest because of the huge and abrupt change in the electrical properties at the transition. Pure vanadium dioxide (VO_2) undergoes a first-order transition from a high-temperature metallic rutile (R) phase to a low-temperature insulating monoclinic ($M1$) one. At the MIT temperature, $T_{MIT}=340$ K, the opening of a band gap in the midinfrared (MIR) region and a jump of several orders of magnitude in the resistivity are observed.[1]

Most of the scientific interest on this compound is focused on understanding the role and the relative importance of the electron-electron correlation and the structural transition in driving the MIT. Despite the remarkable experimental and theoretical efforts devoted to VO_2 during the last 30 years (see, e.g., the review in Ref. 2), the understanding of the MIT is still far from being complete.[3–8]

In the R phase ($T>T_{MIT}$) the V atoms, each surrounded by an oxygen octahedron, form a body-centered tetragonal lattice. Octahedra are arranged in edge-shared strings and consequently the V atoms are equally spaced (V-V distance of 2.88 Å) along linear chains in the c-axis direction.[9] On decreasing temperature below T_{MIT}, the system enters the $M1$ monoclinic insulating phase. In this structure V ions in each chain form pairs along the c axis (V-V distances of 2.63 Å within pairs and 3.16 Å between pairs). In addition each V-V pair is tilted with respect to the c axis, leading to a zigzag pattern. Due to such distortion, a doubling of the unit cell occurs, with space group changing from D_{4h}^{14} (R) to C_{2h}^5 ($M1$).[10]

It is well known that proper chemical substitution of V significantly affects the physical properties of VO_2.[11] While the effects of donor impurities such as W or Nb can be described by conventional extrinsic semiconductor theory,[12,13] acceptor impurities such as Cr or Al have small effects on conductivity but give rise to important structural modifications.[11,14] On doping VO_2 with small amounts of Cr, two additional monoclinic insulating phases, $M2$ and $M3$ (space group C_{2h}^3), mainly characterized by different arrangements of the vanadium chains,[14,15] appear. The $V_{1-x}Cr_xO_2$ phase diagram as a function of the Cr substitution fraction x is shown in Fig. 1, as determined by Marezio *et al.*[14] In $V_{1-x}Cr_xO_2$ T_{MIT} is weakly x dependent, slightly increasing on increasing the Cr content and the MIT is still accompa-

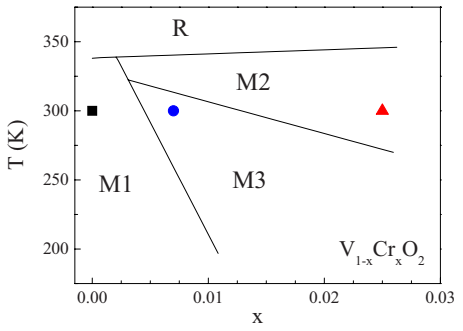

FIG. 1. (Color online) $T-x$(Cr) phase diagram of $V_{1-x}Cr_xO_2$ from Ref. 14. R and $M1$, $M2$, and $M3$ indicate the metallic rutile and the three insulating monoclinic phases, respectively (see text). The solid symbols indicate both the working temperature and the Cr concentration of the three samples investigated in the present work.

nied by a structural transition from the rutile to the monoclinic symmetries. At room temperature (RT) and on increasing x above 0.004, a transition from the $M1$ to the $M3$ monoclinic phase appears. On further increasing the concentration along the room-temperature isotherm, a transition to the $M2$ phase occurs. In the $M2$ structure the dimerization observed in the $M1$ phase is partially removed: one-half of the V atoms dimerizes along the c axis and the other one forms zigzag chains of equally spaced atoms.[14] The $M3$ phase is insulating and has the same space group of $M2$ according to Ref. 14. Other authors reported a small triclinic splitting.[16,17] In this intermediate structure the V-V pairs of the $M2$ phase tilt and the zigzag chains start to pair. From a structural point of view, the $M3$ phase is intermediate between $M1$ and $M2$, so that an almost continuous transition from the $M3$ to the $M1$ phase has been observed on decreasing the temperature.[15] The $M2$ and $M3$ phases, stabilized by very low Cr doping level, slightly differ from the $M1$ phase and can be interpreted as metastable phases for pure VO_2, whose free energy is only slightly larger than that of $M1$.[18]

Within a band theory framework, Goodenough[19] first proposed that the lattice distortion, leading to the R to $M1$ transition (i.e., the V-V pairing and their off-axis zigzag displacement), implies a band splitting with the formation of a Peierls-type gap. The same arguments have been early adopted to describe the MIT also in $M2$ and $M3$ systems.[20] The nonmagnetic nature of the insulating phases supports this scenario, in which VO_2 is an ordinary band (Peierls) insulator. First-principle calculations of the electronic structure based on local-density approximation (LDA) demonstrated the validity of this description, although these calculations failed to yield the opening of the band gap.[21,22] In fact, as early pointed out,[13] the electron-electron correlation has to be taken into account to obtain the insulating phase. Recently, it was shown that, properly accounting for Coulomb repulsion, it is possible to capture correctly both the rutile metallic and monoclinic insulating state of VO_2.[4]

However, the debate on whether the MIT is driven by an electronic or a structural mechanism is still open. The anomalous linear temperature dependence of dc conductivity above T_{MIT} without any sign of saturation up to 800 K,[23] as well as the broad energy range (5 eV) in which the spectral weight is redistributed at the MIT,[7] point out the key role of the electronic correlation in this system. Moreover, the $M2$ phase with its two type of V-V chains can be hardly considered within the band theory framework, where the insulating phase originates from the Peierls pairing. Indeed, in $M2$ phase half of the V atoms forms evenly spaced linear chains that can be regarded as one-dimensional Heisenberg chains according to NMR (Ref. 15) and electron paramagnetic resonance (EPR) (Ref. 17) studies. Despite the band-structure arguments of Goodenough and Hong,[20] the insulating character of the $M2$ phase has been reported as an important support of the idea that the electronic Coulomb repulsion (U) plays a key role in VO_2 and that the physics of this system is close to that of a Mott–Hubbard insulator.[15,18]

In order to gain a deeper understanding of the MIT in pure and Cr-doped VO_2, high-pressure studies have also been carried out. Early resistivity measurements[24] show in pure VO_2 a small pressure-induced *increase* (about 3 K) in T_{MIT} in the 0–4 GPa range. On the contrary the $x=0.025$ Cr-doped sample in the $M2$ phase shows a 20 K decrease in T_{MIT} within the 0–3 GPa range, whereas on further increasing pressure it remains almost constant, ($T_{MIT}\sim 325$ K) up to 5 GPa.[14] This discontinuity has been ascribed to a pressure-induced $M2$ to $M3$ transition. On the basis of these results and of thermodynamics arguments, a pressure temperature phase diagram has been predicted, with a triple point at $P\sim 5$ GPa and $T\sim 325$ K. On applying pressure at room temperature on the $x=0.025$ Cr-doped sample ($M2$ phase), a transition to the $M3$ phase is thus expected at 1.5 GPa.[14]

In a recent high-pressure Raman and MIR study of VO_2,[25] we demonstrated that the MIT and the structural rutile to monoclinic phase transition are decoupled in pure VO_2 at high pressure. A room-temperature monoclinic metallic phase appears indeed accessible in the high-pressure regime ($P>10$ GPa). These results support the hypothesis that the MIT in VO_2 is mainly driven by electronic correlation, although a Peierls contribution cannot be completely ruled out, since a subtle rearrangement of the V-V pairs seems to occur at high pressure (~ 10 GPa).

In the present paper we report the results of a high-pressure Raman study carried out at RT on two samples of $V_{1-x}Cr_xO_2$ family, namely, $x=0.007$ ($M3$ phase at RT and $P=0$) and $x=0.025$ ($M2$ phase at RT and $P=0$). The present Raman results, combined with those reported in Ref. 25 carried out on VO_2 ($x=0$) at RT, allowed us to compare the effect of pressure on VO_2-like systems. Moreover a high-pressure MIR study has been carried out at RT on the sample with the highest doping level ($x=0.025$) to be compared with the results reported in Ref. 25 for pure VO_2.

In Sec. II the growth and characterization of the samples studied and the experimental setup used in our experiments are described. In Secs. III and IV we show ambient pressure and high-pressure Raman spectra, respectively. In Sec. V we describe the MIR measurements. An interpretation of our results is given in Sec. VI.

II. EXPERIMENT

VO_2 was prepared starting from proper amounts of V_2O_3 and V_2O_5 (Aldrich, >99.9%) pressed in form of pellet and

reacted at 1050 °C in an argon flow for 12 h. Small crystals of few tens of micron size have been obtained. $V_{1-x}Cr_xO_2$ samples with $x=0.025$ and $x=0.007$ in the $M2$ and $M3$ monoclinic insulating phase, respectively, at ambient conditions (see phase diagram in Fig. 1) have been synthesized starting from equimolar amounts of V_2O_3 and V_2O_5 and adding proper stoichiometric amounts of Cr_2O_3. The mixture has been fired at 1000 °C under an argon atmosphere. Phase purity was checked through x-ray powder diffraction. Insulator to metal transition temperatures of all the three samples obtained from differential scanning calorimetry (DSC) measurements were in good agreement with literature data.[1,14] We notice that in the synthetic procedure we applied, Cr is most probably present in the 3+ oxidation state, which could give rise to a charge imbalance. Although we are not aware if the compensation mechanism for this charge imbalance is obtained with the creation of oxygen vacancies or by an internal oxidation of V^{4+} to V^{5+}, we believe that the small stoichiometry deviation induced by the Cr reduction does not significantly affect the relevant optical properties of our samples.

A screw clamped opposing-plate diamond-anvil cell (DAC) equipped with 400 μm culet II A diamonds has been used for both Raman and MIR high-pressure experiments. The gaskets were made of a 250 μm thick steel foil with a sample chamber of 130 μm diameter and 40–50 μm height under working conditions. We used NaCl and KBr as pressure transmitting media for Raman and MIR measurements, respectively.[25–27] Pressure was measured *in situ* with the standard ruby fluorescence technique.[28]

Raman measurements have been carried out by means of a confocal-microscope Raman spectrometer, equipped with a 20× objective, a 16 mW He-Ne laser (632.8 nm wavelength), and a 1800 lines/mm grating monochromator with a charge-coupled-device detector. Raman spectra were collected in the backscattering geometry and a notch filter was used to reject the elastic contribution. The low-frequency cutoff of the notch filter prevents to collect reliable spectra below 170 cm^{-1}. Under these experimental conditions we achieved a few micron diameter laser spot on the sample and a spectral resolution of about 3 cm^{-1}. Measurements carried out on Cr-doped samples have been performed on finely milled powder.

High-pressure infrared reflectivity and transmittance data of samples in the DAC have been collected at room temperature exploiting the high brilliance of the SISSI infrared beamline at ELETTRA synchrotron in Trieste.[29] The incident and reflected (transmitted) radiations were focused and collected by a cassegrain-based Hyperion 2000 infrared microscope equipped with a mercury cadmium telluride (MCT) detector and coupled to a Bruker IFS 66v interferometer, which allows us to explore the 750–6000 cm^{-1} spectral range. The 5 μm (VO_2) and 3 μm (Cr-doped sample with $x=0.025$) thick slabs have been obtained by pressing finely milled sample powder between the diamond anvils. The sample slabs have been placed on top of a presintered KBr pellet in the gasket hole.[30] This procedure ensures a clean sample-diamond interface. The slits of the microscope were carefully adjusted to collect transmitted and reflected light from the sample only and kept fixed for all the experiment.

The high brilliance of the light source and the proper sample thickness allow us to measure the intensities reflected, $I_R^S(\omega)$, and transmitted, $I_T^S(\omega)$, at each pressure. Possible misalignments and source intensity fluctuations have been accounted for by measuring the intensity reflected by the external face of the diamond anvil $I_R^{DW}(\omega)$ at each working point. At the end of the pressure run we measured the light intensities reflected by a gold mirror placed between the diamonds $I_R^{Au}(\omega)$ and by the external face of the diamond anvil $I_R'^{DW}(\omega)$. By using the ratio $I_R'^{DW}(\omega)/I_R^{DW}(\omega)$ as a correction function, we achieved the reflectivity $R(\omega)$,

$$R(\omega) = \frac{I_R^S(\omega)}{I_R^{Au}(\omega)} \frac{I_R'^{DW}(\omega)}{I_R^{DW}(\omega)}, \tag{1}$$

and the transmittance $T(\omega)$,

$$T(\omega) = \frac{I_T^S(\omega)}{I_T^{DAC}(\omega)} \frac{I_R'^{DW}(\omega)}{I_R^{DW}(\omega)}, \tag{2}$$

where $I_T^{DAC}(\omega)$ is the transmitted intensity of the empty DAC without gasket and with the anvils in tight contact. The simultaneous measurements of $R(\omega)$ and $T(\omega)$ allow us to extract $n(\omega)$ and $k(\omega)$, the real and the imaginary parts of the complex refractive index of the sample, respectively, and so to obtain the optical conductivity $\sigma_1(\omega)$, as explained in Sec. V.

III. AMBIENT CONDITION RAMAN SPECTRA

The Raman spectrum of monoclinic VO_2 has been widely investigated in several works.[25,31,32] However the symmetry assignment of the phonon peaks is still debated, and the corresponding spatial modes have not been assigned. In our previous paper, on the basis of the comparison with the Raman spectrum of NbO_2,[33] we inferred that the low-frequency Raman peaks of VO_2 should be ascribed to the motions of the V ions only. In order to provide support to this assignment, we performed an oxygen isotope substitution on pure VO_2 and analyzed the effect of the substitution on the Raman spectra. Oxygen stable isotope ^{18}O can be introduced into vanadium oxide by an annealing of the sample in the atmosphere of $^{18}O_2$ (1 bar) at temperatures above 600 °C. At these conditions V_2O_5 phase becomes stable. From V_2O_5, a stoichiometric V_2O_3 has been obtained by a hydrogen reduction. Finally VO_2 has been synthesized by mixing of V_2O_5 and V_2O_3 in the appropriate ratios and annealing at 775 °C for 50 h in a sealed quartz ampoule.

Room-temperature Raman spectra of ^{16}O and ^{18}O VO_2 are shown in Fig. 2 where it is well evident that the isotope substitution leads to a shift of all the phonon peaks, but the two low-frequency modes at ~190 and 220 cm^{-1} (ω_{V_1} and ω_{V_2} in Fig. 2, respectively). The absence of isotope effect on the ω_{V_1} and ω_{V_2} frequencies confirms that these modes can be ascribed to V motion only. On the other hand, the most shifted structure is the peak at ~620 cm^{-1} (ω_O), whose frequency scales with the reduced mass between the oxygen and the vanadium atoms. We notice that a polarization analysis of preliminary Raman measurements carried out on small

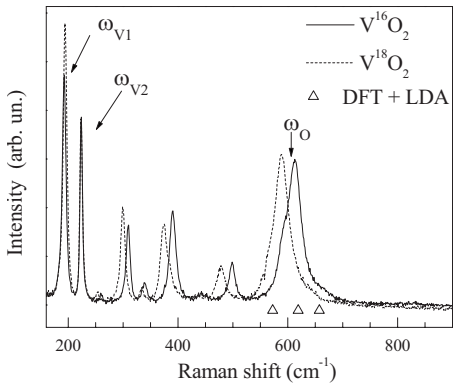

FIG. 2. Room-temperature ambient pressure Raman spectra of ^{16}O and ^{18}O VO_2. The open symbols indicate the frequency value obtained by DFT+LDA calculations on ^{16}O VO_2 (see text) in the high-frequency region.

VO_2 single crystal showed a fine structure of the spectral feature at 620 cm^{-1} which consists of three peaks: a strong central one and two weak shoulders.

The assignment of V-O and V-V modes has been confirmed by a preliminary theoretical calculation of the lattice dynamics carried out within the density functional theory (DFT) under the LDA. The pattern of the frequencies of the Raman-active modes theoretically obtained is in good agreement with the experimental findings. The agreement is particularly good at high frequency, where three Raman-active modes are identified around 600 cm^{-1}, as shown in Fig. 2. Obtained results confirm the assignation of the mode at 620 cm^{-1} to a V-O mode and indicate that this mode mainly involves the oxygen ions connecting the different V chains along the *c* axis. Room-temperature Raman spectra of a pure and $x=0.025$ and $x=0.007$ Cr-doped VO_2 (in the $M2$ and $M3$ phase, respectively) are shown in Fig. 3.

Undoped VO_2 ($M1$) spectrum is in good agreement with previous data.[31,32] Fifteen narrow phonon peaks of the 18 Raman-active modes predicted for the $M1$ phase (9 Ag +9 Bg) have been identified. Similar peak patterns have been observed on $M2$ and $M3$ phases. For the latter structures, group theory predicts the same number of Raman-active phonon modes of $M1$ phase but with different symmetries (10 Ag+8 Bg).

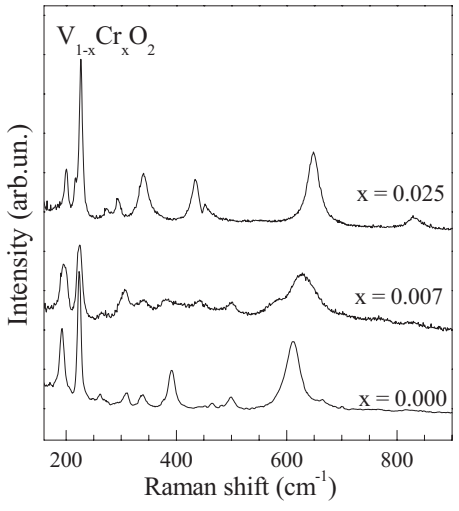

FIG. 3. Room-temperature ambient pressure Raman spectra of $V_{0.975}Cr_{0.025}O_2$ ($M2$), $V_{0.993}Cr_{0.007}O_2$ ($M3$), and pure VO_2 ($M1$).

Great care has been used in order to avoid sample heating during measurement. In particular the laser power has been reduced by 2 orders of magnitude to collect Raman spectrum of $x=0.007$ sample in the $M3$ phase. Indeed, on increasing the laser power (i.e., on increasing the temperature) a reversible transition into the $M2$ phase occurs because of the vicinity of this sample to the $M2$-$M3$ border line at room temperature (see Fig. 1). In this condition this sample shows the same spectrum of $x=0.025$ Cr-doped material. High-temperature ($T>T_{MIT}$) measurements carried out on the two Cr-doped samples and on the parent VO_2 compound show that the Raman spectrum of these samples in the rutile phase (four Raman-active modes) does not show any significative difference.

The phonon frequency shift with respect to the $M1$ modes of pure VO_2 is well evident in the peak at around 600 cm^{-1} (ω_O) and, although much smaller, in the low-frequency mode at ω_{V_1} [this can be hardly seen in Fig. 3, but it is rather evident in Figs. 7(b) and 7(c)]. We notice that the same shift of the ω_O and ω_{V_1} peak observed in $x=0.025$ doped sample has been previously observed in nonstoichiometric VO_2 samples, as reported in Ref. 34. This finding suggests that the presence of V^{3+} or V^{5+} in nonstoichiometric VO_2 stabilizes the $M2$ phase, as well as the Cr impurities.

IV. PRESSURE-DEPENDENT RAMAN SPECTRA

Raman spectra of pure, $x=0.007$ and $x=0.025$, Cr-doped VO_2 samples have been collected as a function of pressure at room temperature. Owing to the tight contact between the sample and the hydrostatic medium and to the high thermal conductivity of diamond, the loading procedure prevents laser-induced sample heating. Measured spectra were fitted by using a standard model curve[26] given by the sum of the phonon contributions, each described by damped harmonic oscillator (DHO), and an electronic contribution,

$$[1+n(\omega)]\left(\frac{B\omega\Gamma}{\omega^2+\Gamma^2}+\sum_{i=1}^{N}\frac{A_i\gamma_i^2\omega_i\omega}{(\omega_i^2-\omega^2)^2+\gamma_i^2\omega_i^2}\right). \quad (3)$$

The parameters B and Γ characterize the electronic response and ω_i, γ_i, and A_i are the frequency, linewidth, and intensity of the ith phonon peak, respectively. The quantity $[1+n(\omega)]$ accounts for the Bose–Einstein statistics. In order to account for the background in the Raman spectra, a linear baseline and the diamond florescence signal at each working point have been included in the fitting curve. A fit example of $P\sim 0$ VO_2 Raman spectrum in the DAC is shown in Fig. 4.

Room-temperature Raman spectra of $x=0.025$ (panel a) and $x=0.007$ (panel b) samples are shown in Fig. 5 at selected pressure. High-pressure Raman spectra of the parent undoped sample collected over a similar pressure range have been reported in our previous work.[25] Background contribution obtained by the fit of the data has been subtracted for clarity. As already observed in the pure compound,[25] high

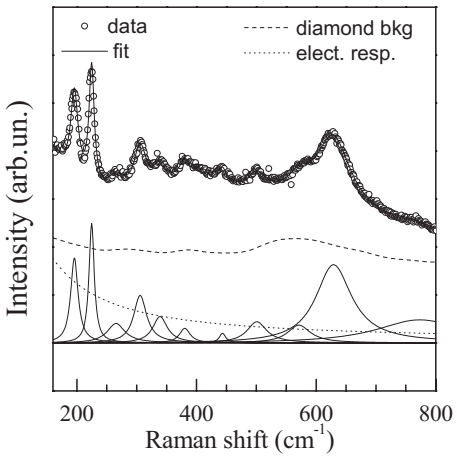

FIG. 4. Room-temperature Raman spectrum of $x=0.007$ Cr-doped sample in the diamond-anvil cell at 0.1 GPa (open circles) and best fit (full line). DHO phonon contributions (full lines), diamond background (dashed line), and electronic response (dot line) have been reported.

pressure does not significantly change the peak pattern and the general spectral shape over the whole pressure range explored. Variation on the relative intensities of phonon peaks must be ascribed to polarization effect.[35] Since the Raman spectrum of the R phase ($T>T_{MIT}$) is completely different from that of the monoclinic phases,[25,32] and accordingly with the results previously obtained on VO_2,[25] we can safely conclude at a glance that a transition to a R phase of the two Cr-doped samples is not achieved within the explored pressure range. On applying pressure on the pure sample a regular hardening of the phonon frequencies has been observed, apart from the change in slope occurring at around 10 GPa in the pressure dependence of the ω_{V_1} and ω_{V_2} peaks.[25] The effect of pressure on the present $x=0.025$ and $x=0.007$ Cr-doped samples appears more complex and somehow unexpected. Indeed, on increasing the pressure the Raman spectra

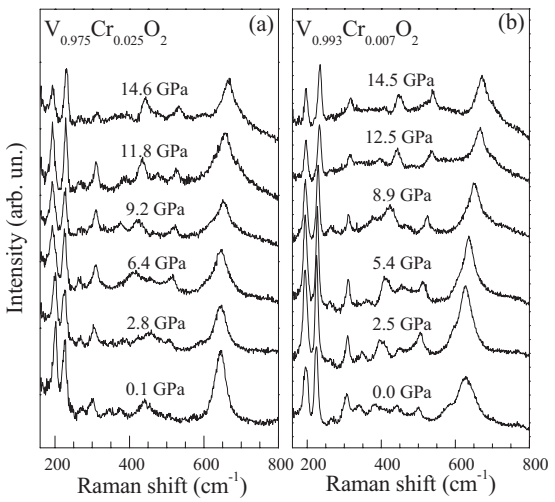

FIG. 5. Room-temperature Raman spectra of (a) $x=0.025$ and (b) $x=0.007$ Cr-doped VO_2 at selected pressure. Diamond background obtained by the fitting procedure has been subtracted for clarity.

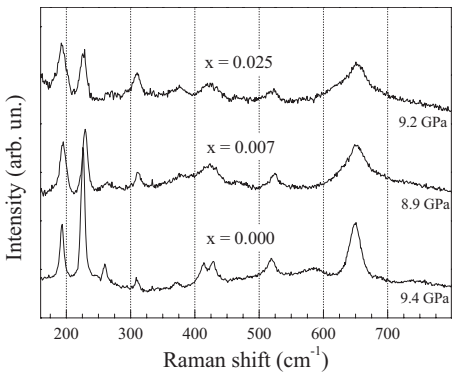

FIG. 6. Comparison between room-temperature Raman spectra of pure VO_2, and $x=0.025$ and $x=0.007$ Cr-doped VO_2 at $P\simeq 9$ GPa. The dashed lines are guide for the eyes.

of Cr-doped VO_2 gradually evolve toward that of the undoped sample: all the phonon frequency values of the undoped and doped VO_2 are actually coincident at $P\sim 9$ GPa, as shown in Fig. 6.

This finding is confirmed by the results obtained applying the fitting procedure described above. In the following we will discuss the best-fit results obtained for the ω_{V_1}, ω_{V_2}, and ω_O phonon modes, since they give the most relevant information about the V-V and V-O motions, as discussed in Sec. II. The obtained phonon frequencies of the ω_{V_1}, ω_{V_2}, and ω_O phonon modes are shown in Fig. 7 as a function of pressure together with those previously achieved for VO_2.[25]

Cr-doped samples, as well as the parent compound, show a remarkable pressure dependence of all the phonon peaks. In particular, the high-frequency mode ω_O is almost pressure independent up to ~ 9 and ~ 3 GPa for the $x=0.007$ ($M3$)

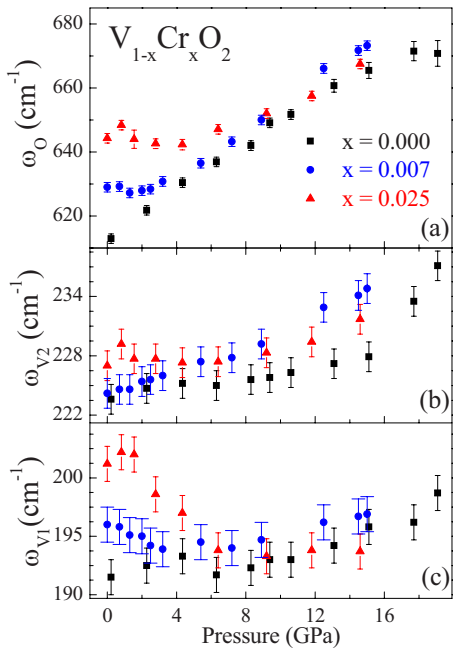

FIG. 7. (Color online) VO_2 (black full square) and $x=0.025$ and $x=0.007$ Cr-doped sample (red triangles and blue circles, respectively) phonon frequencies of (a) the V-O and [(b) and (c)] the V-V modes as a function of pressure.

and the $x=0.025$ ($M2$) samples, respectively, where it approaches the values obtained for pure VO_2 ω_O. On further increasing the pressure the three samples show actually the same pressure dependence [Fig. 7(a)]. The behavior of the low-frequency mode ω_{V_1} is even more interesting, showing a clear softening of the phonon frequencies down to the pure VO_2 ω_{V_1} value at 8–9 and 3–4 GPa for the $x=0.025$ ($M2$) and the $x=0.007$ ($M3$) samples, respectively [Fig. 7(b) and Fig. 7(c)]. The ω_{V_2} peak of the three samples shows instead a rather similar pressure dependence over all the pressure range.

These findings indicate a gradual transition in $x=0.025$ and $x=0.007$ Cr-doped samples from the $M2$ and $M3$ structure, respectively, to that shown by VO_2 ($M1$) at high pressure. Finally the change in slope of the pressure dependence of ω_{V_1} and, albeit less evident, of ω_{V_2} observed at around 10 GPa in all the three samples suggests a common subtle rearrangements of the V chains.

V. PRESSURE-DEPENDENT INFRARED MEASUREMENTS

In order to compare the results previously obtained for pure VO_2 ($M1$),[25] high-pressure midinfrared reflectivity $R(\omega)$ and transmittance $T(\omega)$ spectra of the $x=0.025$ sample ($M2$) have been collected with the experimental setup described in Sec. II and in Ref. 25. Present results for the Cr-doped sample together with those for VO_2 are shown in Fig. 8 at selected pressure.

At ambient pressure the low-frequency reflectivity of the Cr-doped sample is characterized by a steep phononic absorption, whereas, on increasing frequency, $R(\omega)$ is almost flat. The interference fringes, well evident in both $R(\omega)$ and $T(\omega)$ originate by the multiple reflections within the sample-KBr bilayer. The low $T(\omega)$ values in the high-frequency side of the graph are due to the absorption of the low-frequency tail of the electronic band. Data are not shown in the 1600–2700 cm^{-1} range, where the multiphonon diamond absorption prevents data reliability. The bump at about 3500 cm^{-1} is due to a bad compensation of the diamond absorption in this region.

On increasing pressure, $R(\omega)$ does not change remarkably up to 10 GPa, whereas $T(\omega)$ gradually decreases. On further increasing the pressure, $R(\omega)$ starts to increase and $T(\omega)$ is strongly reduced due to the shift of the electronic band toward lower frequencies. A clear evidence of this process is found in the optical density $O_d(\omega)=-\ln T(\omega)$ shown in the inset of Fig. 8. The electronic contribution fills the optical gap and remarkably screens the phonon peak revealing a pressure-induced carrier delocalization. The comparison with the data collected on VO_2 (Ref. 25) shows that both $R(\omega)$ and $T(\omega)$ exhibit similar ambient pressure spectra, as well as similar pressure dependence.

A careful analysis of the data allows us to achieve a deeper understanding about the observed effect. Exploiting the simultaneous measurements of $R(\omega)$ and $T(\omega)$, we can extract $n(\omega)$ and $k(\omega)$, the real and the imaginary parts of the complex refractive index of the sample, respectively. To this purpose a multilayer scheme diamond-sample-KBr diamond has been adopted taking into account the multiple reflections

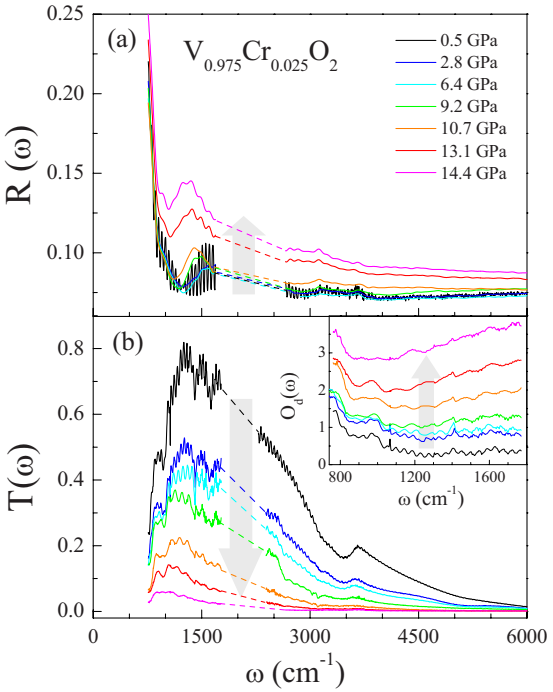

FIG. 8. (Color online) (a) MIR reflectivity $R(\omega)$ and (b) transmittance $T(\omega)$ of $x=0.025$ Cr-doped VO_2 at selected pressures. The arrows indicate increasing pressure. Data have been cut in the diamond absorption frequency range. The dashed lines are guides for the eyes. For sake of clarity, fringes have been averaged out in the reflectivity spectra, except at the lowest pressure. Inset: low-frequency optical density $O_d(\omega)$.

within the sample and the KBr layers by adding incoherently the intensities of the reflected beams.[36] Knowing the slab thickness d, the refractive index of diamond,[37] and the optical properties of KBr as a function of pressure,[38] we had to solve a nonanalytical system of two equations for each frequency to obtain the real and the imaginary parts of the sample complex refractive index, $n(\omega)$ and $k(\omega)$, respectively. We solved this system by a numerical iteration technique. To initialize the iterative procedure the guess function $n^0(\omega)$ was set equal to the average refraction index $\langle n\rangle$ of room-temperature VO_2 (from Ref. 39) and $k^0(\omega)$ is obtained inserting $n^0(\omega)$ into the $T(\omega)$ equation. The subsequent iteration, $n^1(\omega)$, is obtained inserting $k^0(\omega)$ into $R(\omega)$ and in turn $n^1(\omega)$ into $T(\omega)$ to get $k^1(\omega)$. The iteration procedure rapidly converges giving results stable within 1% after few steps. This procedure has been previously adopted in analyzing the infrared data collected on VO_2 and the resulting $n(\omega)$ and $k(\omega)$ at the lowest pressure were found to be in good agreement with the ambient pressure data reported in the literature.[7,39] We point out that we have checked the independence of the results from the guess function and that a complete agreement is found when a different calculation technique[6] is adopted to obtain $n(\omega)$ and $k(\omega)$.

From $n(\omega)$ and $k(\omega)$, the optical conductivity $\sigma_1(\omega)=2\omega/4\pi n(\omega)k(\omega)$ of the Cr-doped sample have been calculated at each pressure and shown in Fig. 9. The results reported in Ref. 25 are also shown for sake of comparison. The low-frequency region of the spectra has not been reported

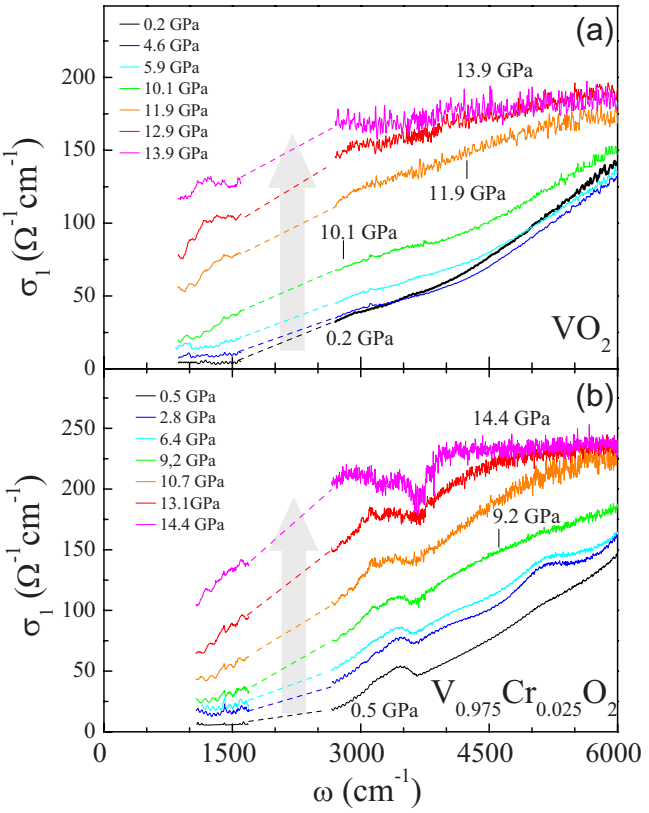

FIG. 9. (Color online) (a) Optical conductivity $\sigma_1(\omega)$ of undoped VO_2 from Ref. 25 and (b) $x=0.025$ Cr-doped VO_2 as a function of pressure. The dashed lines are guide for the eyes.

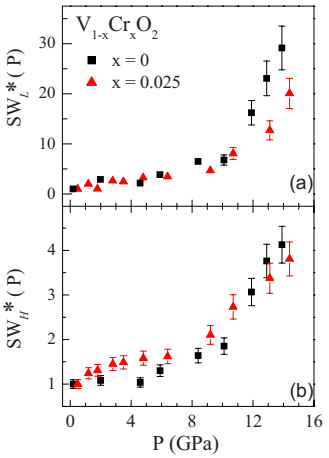

FIG. 10. (Color online) Normalized spectral weights as function of pressure of undoped VO_2 (black squares) from Ref. 25 and $x=0.025$ Cr-doped VO_2 (red triangles) calculated in the low frequency (900–1600 cm^{-1}) and in the high-frequency (2600–5000 cm^{-1}) regions.

because the strong variations of the optical constants around the phonon contribution could affect the reliability of the results of the iterative procedure. In any case the investigated spectral region allows us to follow the pressure behavior of the low-frequency tail of the electronic band, which is the spectral structure mostly affected by the MIT.[7]

On increasing pressure, VO_2 shows a weakly pressure dependent $\sigma_1(\omega)$ up to 4 GPa, whereas on further increasing the pressure, $\sigma_1(\omega)$ progressively increases, mainly within the 1500–4500 cm^{-1} frequency range. Above 10 GPa an abrupt increase in the overall $\sigma_1(\omega)$ occurs and a remarkable pressure-induced band-gap filling is observed. On increasing pressure in Cr-doped sample a similar $\sigma_1(\omega)$ behavior is observed, characterized by a gap filling, but $\sigma_1(\omega)$ starts to increase already on applying relatively small pressure. At high pressure ($P>10$ GPa) the optical conductivity has the same shape of that observed in the undoped sample. It is worth to notice that highest-pressure data show that the energy gap of both the samples, if still open, is well below 1000 cm^{-1}. A rough linear extrapolation of the data collected at $P>10$ GPa gives positive, although small, $\sigma_1(\omega=0)$ values, compatible with a bad metal behavior.

Following the same procedure adopted in Ref. 25, the effect of pressure can be better visualized if the pressure dependence of the spectral weight is analyzed. At each pressure we calculated the integral of $\sigma_1(\omega)$ over the 1050–1700 cm^{-1} and 2700–5000 cm^{-1} frequency ranges, called $SW_L(P)$ and $SW_H(P)$, respectively. The integration has not been extended to the frequency region above 5000 cm^{-1}, owing to the onset of saturation effects in the spectra collected at the highest pressures (see in Fig. 8 the high noise level of these spectra at high frequencies). The spectral weights normalized to the lowest-pressure values, $SW_L^*(P)=SW_L(P)/SW_L(0)$ and $SW_H^*(P)=SW_H(P)/SW_H(0)$, have been calculated. Present results in comparison with those reported in Ref. 25 for VO_2 are shown in Fig. 10. Low- and high-frequency spectral weights show the same pressure dependence, with a rather abrupt change in slope which remarkably occurs at 10 GPa in both the samples. We notice that the absolute pressure-induced variation of $SW_L(P)$ is much larger than that observed for $SW_H(P)$ as expected if charge delocalization occurs.[7] Such a large and abrupt increase in the spectral weight in the gap region is certainly compatible with the occurrence of a pressure-induced MIT, although the spectral range of the present measurements does not allow us to claim undoubtedly the complete optical gap closure above 10 GPa. We want to finally notice that the absolute values of the normalized spectral weight are almost the same for both samples, whereas, differently from the pure VO_2, in the Cr-doped sample a slight increase can be seen also at low pressure.

VI. DISCUSSION AND CONCLUSIONS

The present results together with those reported in Ref. 25 allow for a careful analysis of the effects of the different monoclinic distortions on both the lattice and the electronic dynamics of pure and Cr-doped VO_2 under pressure. The regular pressure dependence of the VO_2 phonon peaks (see Fig. 7) indicates the stability of the $M1$ phase at least up to 10 GPa whereas, on the contrary, the anomalous pressure behavior of the Raman-active phonon peaks of the Cr-doped compounds shows a low-pressure structural instability of the $M2$ and $M3$ phases. The peak patterns of the Raman-active phonon of the three monoclinic phases ($M1$, $M2$, and $M3$)

remarkably differ at ambient pressure but, on applying pressure, the whole spectrum of the two Cr-doped compounds evolves toward the spectrum shown by the pure compound at high pressure (see Fig. 6). The transition is continuous and extends over a wide pressure range being completed at $P \sim 3$ GPa and at $P \sim 9$ GPa for the $x=0.007$ ($M3$) and $x=0.025$ ($M2$) Cr-doped samples, respectively. Since present ambient pressure measurements show that Raman spectroscopy is very sensitive to the different monoclinic phases (see Fig. 3), these results indicate that the three systems are in the same lattice configuration above 9 GPa. Moreover, since the Raman phonon frequencies of the $x=0.007$ ($M3$) and $x=0.025$ ($M2$) Cr-doped samples keep significantly different at least up to 9 GPa, our data do not confirm the $M2$ to $M3$ structural transition at ~1.5 GPa (Ref. 14) claimed for the $x=0.025$ sample. We just notice a weak anomaly in the low-pressure behavior of the three phonon peaks of the $x=0.025$ Cr-doped sample shown in Fig. 7.

As discussed in Sec. I, the three monoclinic phases differ for the V ion pairing and the tilting of the V-V pairs which causes an off-center displacement of the V ions. This produces a general distortion of the oxygen octahedral cage leading to different V-O bond lengths within the same octahedron and, in Cr-doped samples, also between the two classes of octahedra. To make a rough comparison among the three monoclinic structures, an average volume per octahedron can be calculated from the average equatorial and apical V-O bond lengths using the available data.[14] Following this procedure we obtain almost equal octahedron volumes for $M1$ and $M3$ phases whereas the average volume is slightly larger for the $M2$ phase (about 0.5%). Moreover, following Ref. 14 a measure of the octahedral distortion can be provided by the standard deviation of the V-O distances from the average value. The result is that the octahedral distortion decreases on going from $M2$ to $M3$ to $M1$.[14] Bearing in mind these findings, the peculiar pressure dependence shown by the ω_O phonon of the three samples can be ascribed to a progressive compression and symmetrization of the octahedra. Indeed on applying pressure, $M3$ (intermediate distortion, minimum volume) transforms into $M1$ (minimum distortion, minimum volume) at ~3 GPa, whereas $M2$ (maximum distortion, maximum volume) transforms into $M1$ at a much higher pressure (~9 GPa). On further increasing the pressure, the change in slope in the pressure dependence of the V mode shown by all the three samples above 10 GPa [see Fig. 7(c)] suggests a slight rearrangement of the V chains, leading to a common monoclinic phase (M_x), where the extent of the Peierls distortion is still unknown.

The comparison between the infrared data of pure and $x=0.025$ Cr-doped VO_2 shows that the partial removal of the V-V dimerization, characteristic of the $M2$ phase, does not sensibly affect the low-frequency electronic properties, since the two samples show rather similar low-frequency optical conductivity [$\sigma_1(\omega)$]. Also the $\sigma_1(\omega)$ pressure behaviors are quite similar in the two samples, except for slight differences in the spectral weights at low pressure (see Fig. 10). Two regimes below and above a threshold pressure $P^* \sim 10$ GPa can be clearly identified in both the samples. While for $P < P^*$ a weak pressure dependence in optical conductivity is observed (see Figs. 9 and 10), for $P > P^*$ a clear charge delocalization process occurs, quite remarkable at the highest pressures. The spectral shape and the $\sigma_1(\omega)$ values at low frequency at highest pressures show the achieving of a bad metallic behavior. Bearing in mind the Raman data, the whole of these results indicates that, on increasing pressure, Cr-doped VO_2 enters the same M_x structure of the high-pressure pure VO_2, in which the pressure enables a metallization process.

Combining high-pressure Raman and infrared results, we can outline an unexpected regime for room-temperature pure and Cr-doped VO_2 at high pressure, where the monoclinic to rutile and the insulator to metal transitions are decoupled. Indeed, the observed pressure-induced metallization process occurs within the monoclinic lattice symmetry, which retains well above 15 GPa (at least up to 19 GPa for VO_2). Preliminary high-pressure x-ray diffraction measurements[40] extend the stability of the monoclinic symmetry for VO_2 up to 42 GPa, giving further support the above statement. Furthermore the same structural data show an abrupt reduction in the volume of the unit cell on increasing pressure above 10 GPa,[40] indicating the occurrence of a lattice instability within the monoclinic symmetry, here conjectured on the basis of Raman results.

Since the monoclinic lattice symmetry is the structural signature of Peierls lattice distortions, the present results support a major role of the electron correlations against structural effects (Peierls charge-lattice coupling) in driving the system toward a metallic phase. The discontinuity shown by the low-frequency V-V modes ω_{V_1} and ω_{V_2} at P^* (see Fig. 7) suggests a subtle rearrangement of the V-V chains which may play a role in driving the system toward a metallic phase. Nevertheless, since the large lattice distortion from the $M1$ phase shown by the $M3$ and $M2$ phases does not induce sensible effects on the electronic properties of these systems, we can guess that the onset of the metallization in all the investigated samples is mainly related to the electronic correlation and not to the lattice dynamics. On the other hand, recent results obtained on pure VO_2 confirm the relevance of electronic correlation on the MIT and a Mott transition within an insulator/metallic phase-coexistence scenario has been indeed revealed.[8]

In summary, we have reported on a high-pressure Raman and infrared investigation on two Cr-doped VO_2 compounds. We pointed out the presence of a common high-pressure monoclinic lattice structure M_x. Differently from ambient pressure, where the metallic phase is shown only in conjunction with the rutile structure (slightly above RT), a metallic phase appears accessible at room temperature in the high-pressure regime of the monoclinic M_x phase. Although this transition seems to be related also to subtle rearrangements of the V-V chains, the comparison of the effect of pressure on samples with different extents of Peierls distortion supports a major role of the electron correlations against charge-lattice coupling. The present results thus open to new experimental queries and represent a severe benchmark for theoretical model aimed at addressing the role of the electron-electron correlation and the structural transition in driving the MIT in VO_2.

[1] F. J. Morin, Phys. Rev. Lett. **3**, 34 (1959).
[2] M. Imada, A. Fujimori, and Y. Tokura, Rev. Mod. Phys. **70**, 1039 (1998).
[3] H. T. Kim, B. G. Chae, D. H. Youn, S. L. Maeng, G. Kim, K. Y. Kang, and Y. S. Lim, New J. Phys. **6**, 52 (2004).
[4] S. Biermann, A. Poteryaev, A. I. Lichtenstein, and A. Georges, Phys. Rev. Lett. **94**, 026404 (2005).
[5] M. W. Haverkort, Z. Hu, A. Tanaka, W. Reichelt, S. V. Streltsov, M. A. Korotin, V. I. Anisimov, H. H. Hsieh, H.-J. Lin, C. T. Chen, D. I. Khomskii, and L. H. Tjeng, Phys. Rev. Lett. **95**, 196404 (2005).
[6] H. S. Choi, J. S. Ahn, J. H. Jung, T. W. Noh, and D. H. Kim, Phys. Rev. B **54**, 4621 (1996).
[7] M. M. Qazilbash, K. S. Burch, D. Whisler, D. Shrekenhamer, B. G. Chae, H. T. Kim, and D. N. Basov, Phys. Rev. B **74**, 205118 (2006).
[8] M. M. Qazilbash, M. Brehm, B.-G. Chae, P.-C. Ho, G. O. Andreev, B.-J. Kim, S. J. Yun, A. V. Balatsky, M. B. Maple, F. Keilmann, H.-T. Kim, and D. N. Basov, Science **318**, 1750 (2007).
[9] D. B. McWhan, M. Marezio, J. P. Remeika, and P. D. Dernier, Phys. Rev. B **10**, 490 (1974).
[10] J. M. Longo and P. Kierkegaard, Acta Chem. Scand. (1947-1973) **24**, 420 (1970).
[11] J. M. Reyes, M. Sayer, A. Mansingh, and R. Chen, Can. J. Phys. **54**, 413 (1976).
[12] J. M. Reyes, M. Sayer, and R. Chen, Can. J. Phys. **54**, 408 (1976).
[13] A. Zylbersztejn and N. F. Mott, Phys. Rev. B **11**, 4383 (1975).
[14] M. Marezio, D. B. Mc Whan, J. P. Remeika, and P. D. Dernier, Phys. Rev. B **5**, 2541 (1972).
[15] J. P. Pouget, H. Launois, T. M. Rice, P. Dernier, A. Gossard, G. Villeuve, and P. Hagenmuller, Phys. Rev. B **10**, 1801 (1974).
[16] G. Villeneuve, M. Drillon, and P. Hagenmuller, Mater. Res. Bull. **8**, 1111 (1973).
[17] J. P. D'Haenens, D. Kaplan, and P. Merenda, J. Phys. C **8**, 2267 (1975).
[18] T. M. Rice, H. Launois, and J. P. Pouget, Phys. Rev. Lett. **73**, 3042 (1994).
[19] J. B. Goodenough, J. Solid State Chem. **3**, 490 (1971).
[20] J. B. Goodenough and H. Y.-P. Hong, Phys. Rev. B **8**, 1323 (1973).
[21] R. M. Wentzcovitch, W. W. Schulz, and P. B. Allen, Phys. Rev. Lett. **72**, 3389 (1994).
[22] V. Eyert, Ann. Phys. (N.Y.) **11**, 650 (2002).
[23] P. B. Allen, R. M. Wentzcovitch, W. W. Schulz, and P. C. Canfield, Phys. Rev. B **48**, 4359 (1993).
[24] C. N. Berglund, C. N. Berglund and A. Jayaraman, Phys. Rev. **185**, 1034 (1969).
[25] E. Arcangeletti, L. Baldassarre, D. Di Castro, S. Lupi, L. Malavasi, C. Marini, A. Perucchi, and P. Postorino, Phys. Rev. Lett. **98**, 196406 (2007).
[26] A. Congeduti, P. Postorino, E. Caramagno, M. Nardone, A. Kumar, and D. D. Sarma, Phys. Rev. Lett. **86**, 1251 (2001).
[27] A. Congeduti, P. Postorino, P. Dore, A. Nucara, S. Lupi, S. Mercone, P. Calvani, A. Kumar, and D. D. Sarma, Phys. Rev. B **63**, 184410 (2001).
[28] H. K. Mao, P. M. Bell, J. W. Shaner, and D. J. Steinberg, J. Appl. Phys. **49**, 3276 (1978).
[29] S. Lupi, A. Nucara, A. Perucchi, P. Calvani, M. Ortolani, L. Quaroni, and M. Kiskinova, J. Opt. Soc. Am. B **24**, 959 (2007).
[30] A. Sacchetti, M. Cestelli Guidi, E. Arcangeletti, A. Nucara, P. Calvani, M. Piccinini, A. Marcelli, and P. Postorino, Phys. Rev. Lett. **96**, 035503 (2006).
[31] R. Srivastava and L. L. Chase, Phys. Rev. Lett. **27**, 727 (1971).
[32] P. Schilbe, Physica B (Amsterdam) **316**, 600 (2002).
[33] Y. Zhao, Z. Zhang, and Y. Lin, J. Phys. D **37**, 3392 (2004).
[34] Y. Hong-Tao, F. Ke-Cheng, W. Xue-Jin, L. Chao, H. Chen-Jauna, and N. Yu-Xin, Chin. Phys. **13**, 82 (2004).
[35] A. G. Aronov, D. N. Mirlin, I. I. Reshina, and F. A. Chudnovskii, Sov. Phys. Solid State **19**, 110 (1977).
[36] M. Dressel and G. Grüner, *Electrodynamics of Solids* (Cambridge University Press, Cambridge, 2002).
[37] *Handbook of Optical Constants of Solids II*, edited by E. D. Palik (Academic, San Diego, 1991).
[38] P. G. Johannsen, G. Reiss, U. Bohle, J. Magiera, R. Muller, H. Spiekermann, and W. B. Holzapfel, Phys. Rev. B **55**, 6865 (1997).
[39] W. Hans Verleur, A. S. Barker, Jr., and C. N. Berglund, Phys. Rev. **172**, 788 (1968).
[40] M. Baldini and L. Malavasi (unpublished).